PHYSICAL REVIEW C **70**, 031001(R) (2004)

Four-body calculation of the first excited state of ^{4}He using a realistic *NN* interaction: ^{4}He$(e,e')^4$He(0_2^+) and the monopole sum rule

E. Hiyama
Department of Physics, Nara Women's University, Nara 630-8506, Japan

B. F. Gibson
Theoretical Division, Los Alamos National Laboratory, Los Alamos, New Mexico 87545, USA

M. Kamimura
Department of Physics, Kyushu University, Fukuoka 812-8581, Japan
(Received 25 May 2004; published 21 September 2004)

^{4}He possesses a second 0^+ state; the transition form factor has been measured via inelastic electron scattering. The nature of the 0_2^+ state's spatial structure has been controversial. An accurate four-nucleon calculation utilizing a realistic *NN* force (Argonne V8′) plus phenomenological *NNN* three-body force has been performed for both the ^{4}He ground state and second 0^+ state (E_x=20.21 MeV) using the Gaussian expansion method. The calculated one-body densities and transition density show a significant difference between the states. The resulting impulse approximation transition form factor ^{4}He$(e,e')^4$He(0_2^+) agrees with the available data. The overlap of the 0_2^+ wave function with the trinucleon ground state suggests that the structure is primarily a loosely bound $3N+N$ system and not a breathing mode. It is found that a major part of the energy-weighted $E0$ sum rule value is exhausted by nonresonant, low-energy continuum states other than the second 0^+ state, in contrast to heavier nuclei where a dominant fraction of the sum-rule limit is exhausted by the second 0^+ state because it corresponds to a collective, breathing mode.

DOI: 10.1103/PhysRevC.70.031001 PACS number(s): 21.45.+v, 27.10.+h, 25.30.Dh, 21.10.Gv

I. INTRODUCTION

The ^{4}He nucleus is the lightest nucleus that exhibits excited states (resonances). The first excited state (0_2^+) at E_x =20.21 MeV has the same spin, isospin, and parity as the ground state. Therefore, the 0_2^+ state should have quite a different spatial structure in order to be orthogonal to the 0_1^+ state. The second 0^+ state in ^{4}He is then the smallest system in which one can study nuclear spatial excitation using realistic interactions.

In an electron-scattering experiment Frosch *et al.* [1,2] obtained the inelastic scattering cross section (hence, the transition form factor) for the 0^+ excitation of the α particle. Later experiments by Walcher [3] and by Koebschall *et al.* [4] confirmed the measurement. (Halderson *et al.* [5] provide a succinct discussion of the relationship among the published inelastic-scattering cross sections and transition form factors.) The question of the nature of the structure of the ^{4}He 0_2^+ state has since been the subject of numerous theoretical studies.

One of the important tasks in few-body nuclear physics has been to solve the four-nucleon bound-state problem (^{4}He) using realistic *NN* interactions. A benchmark calculation was reported in Ref. [6] by 18 co-authors including two of the present authors (E.H. and M.K.). Seven different few-body research groups solved for the ^{4}He ground state using a realistic interaction, the Argonne V8′ potential (AV8′) [7]. Agreement between the results of the significantly different calculational schemes was essentially perfect in terms of the binding energy, the rms radius, and the two-body correlation function. One of the next challenging projects is to calculate properties of the second 0^+ state of ^{4}He using realistic interactions. One must reproduce simultaneously the ground state and the excited state which have the same spin, isospin, and parity, but possess quite different spatial structure.

In investigating the spatial structure of the ^{4}He 0_2^+ state, it is particularly important to explain the observed (e,e') transition form factor. Moreover, from analyzing the low-momentum-transfer part of the form factor, it was reported that only about 11% of the energy-weighted (EW) $E0$ sum-rule limit was exhausted by the second 0^+ state [3]. In medium-heavy or heavy nuclei, normally 80%–90% of the limit is exhausted by the second 0^+ state because it is a collective, breathing mode. For the ^{4}He nucleus, one should understand where the major component of the sum-rule value is situated.

The ^{4}He experimental and theoretical situation was summarized by Tilly *et al.* [8]. Within the past six years, several calculations pertaining to the structure of the 0^+ excited state of ^{4}He have been reported. Hofmann and Hale explored the system in a $3N+N$ resonating group model (RGM) calculation [9] based upon an early *NN* Bonn potential. Despite the omission of an *NNN* three-body force needed to reproduce the ground-state energy, the authors concluded that it was unlikely that the 0^+ excited state was a breathing mode. Csótó and Hale also performed an RGM calculation [10] using a phenomenological effective *NN* force. The ground state was slightly overbound without the inclusion of an *NNN* force, although the radius was found to be larger than the experimental value. The authors concluded that their best model result implied a resonance at 93 keV above the ^{3}H $+p$ threshold.

Recently, a four-nucleon calculation of the second 0^+ state using the AV8′ potential was performed by Navrátil and Barrett [11] using the no-core shell model. The authors state that the results for the 0_2^+ state and transition form factor obtained within the limited model space should be viewed with some caution. Indeed, the energy of their 0_2^+ state lies some 4 MeV above the energy obtained by our calculation (see below), and their (e,e') form factor, $|F_{\rm inel}|^2$, is approximately three times larger than the observed one. One needs a much larger model space to describe the spatially defuse structure of the 0_2^+ state and reduce the $0_1^+ \rightarrow 0_2^+$ transition form factor.

Most recently, Fonseca *et al.* [12] reported a calculation of the 0_2^+ state using the AGS equations to explore the model dependence for several realistic potentials. Without including a Coulomb force, they obtained two 0^+ bound states, the 0_2^+ state lying 0.02–0.04 MeV below the coincident $n+{}^3$He and $p+{}^3$H thresholds.

One may conclude that proper inclusion of a Coulomb force and an *NNN* force in a realistic *NN* force Hamiltonian is required to obtain a realistic description of the ^{4}He ground and the first excited states simultaneously. Furthermore, a sufficiently large four-nucleon function space is necessary in order to solve the puzzle of where the major component of the monopole sum-rule value is situated.

Therefore, we have performed a full four-body calculation of the 0_1^+ and 0_2^+ states and the monopole sum rule using the Gaussian expansion method (GEM), which was proposed by the Kyushu group some 15 years ago [13,14] and has been successfully used in the study of various three- and four-body systems, including the above-mentioned four-body benchmark calculation of ^{4}He, four-body calculations of light hypernuclei, and Coulomb three-body calculations of reactions of muon-atomic systems (see the review of GEM [15] plus the references therein).

Strictly speaking, the second 0^+ state (E_x=20.21 MeV) is a resonance lying above the $^3\mathrm{H}+p$ threshold (E_x =19.815 MeV) and, therefore, a scattering boundary condition is needed to solve for the wave function. However, it lies below both the top of the $^3\mathrm{H}+p$ Coulomb barrier ($\sim$0.88 MeV) and the $^3\mathrm{He}+n$ threshold (E_x=20.578 MeV), located almost at the mean position (E_x=20.20 MeV) of the two thresholds. The width of this *s*-wave resonance is rather small (500 keV). Therefore, it is acceptable to solve for the wave function using a bound-state boundary condition in an isospin basis where a pure T=0 configuration is assumed. Indeed, we used this framework in the present calculation and obtained the T=0, 0_2^+ state as a bound state below the calculated T=0 (averaged) threshold. This approximate treatment of the asymptotic behavior of the 0_2^+ state is, thus, reasonable so long as one is discussing the $^4\mathrm{He}(e,e')^4\mathrm{He}(0_2^+)$ transition from the ground state, which has a short-range tail.

In Sec. II we briefly explain our GEM calculational method. Interactions employed in the present calculation are discussed in Sec. III. Calculated results are presented in Sec. IV.

II. METHOD

We employ an isospin basis, rather than a neutron-proton (particle) basis, and assume T=0 configurations for the 0_1^+ and 0_2^+ states of ^{4}He. In the GEM approach, the four-nucleon wave function is written as a sum of the component functions in Jacobi coordinates for the rearrangement channels (Fig. 1) within the *LS* coupling scheme,

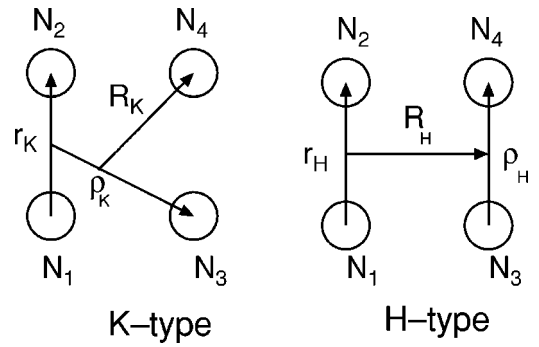

FIG. 1. Jacobian coordinates for the rearrangement channel of ^{4}He. The four nucleons are antisymmetrized.

$$\Psi_{J=0^+} = \sum_\alpha C_\alpha^{(\mathrm{K})} \Phi_\alpha^{(\mathrm{K})} + \sum_\alpha C_\alpha^{(\mathbf{H})} \Phi_\alpha^{(\mathrm{H})}, \tag{2.1}$$

where the antisymmetrized basis functions $\Phi_\alpha^{(\mathrm{K})}$ and $\Phi_\alpha^{(\mathrm{H})}$ are described by

$$\begin{aligned}\Phi_\alpha^{(\mathrm{K})} = \mathcal{A}[&(\{[\phi_{nl}^{(\mathrm{K})}(\mathbf{r}_\mathrm{K})\varphi_{\nu\lambda}^{(\mathrm{K})}(\rho_\mathrm{K})]_\Lambda \psi_{NL}^{(\mathrm{K})}(\mathbf{R}_\mathrm{K})\}_I \\ &\times \{[\chi_s(12)\chi_{1/2}(3)]_{s'}\chi_{1/2}(4)\}_S)_{JM} \\ &\times \{[\eta_t(12)\,\eta_{1/2}(3)]_{1/2}\,\eta_{1/2}(4)\}_0],\end{aligned} \tag{2.2}$$

$$\begin{aligned}\Phi_\alpha^{(\mathrm{H})} = \mathcal{A}[&(\{[\phi_{nl}^{(\mathrm{H})}(\mathbf{r}_\mathrm{H})\varphi_{\nu\lambda}^{(\mathrm{H})}(\rho_\mathrm{H})]_\Lambda \psi_{NL}^{(\mathrm{H})}(\mathbf{R}_\mathrm{H})\}_I \\ &\times [\chi_s(12)\chi_{s'}(34)]_S)_{JM}[\eta_t(12)\,\eta_t(34)]_0],\end{aligned} \tag{2.3}$$

with $\alpha \equiv \{nl,\nu\lambda,\Lambda,NL,I,s,s',S,t\}$. $\mathcal{A}$ is the four-nucleon antisymmetrizer. The χ's and η's are the spin and isospin functions, respectively. The functions $\phi_{nl}(\mathbf{r})$, $\varphi_{\nu\lambda}(\boldsymbol{\rho})$, and $\psi_{NL}(\mathbf{R})$ are taken to be Gaussian basis functions,

$$\begin{aligned}\phi_{nlm}(\mathbf{r}) &= N_{nl} r^l e^{-(r/r_n)^2} Y_{lm}(\hat{\mathbf{r}}), \\ \varphi_{\nu\lambda\mu}(\boldsymbol{\rho}) &= N_{\nu\lambda} \rho^\lambda e^{-(\rho/\rho_\nu)^2} Y_{\lambda\mu}(\hat{\boldsymbol{\rho}}), \\ \psi_{NLM}(\mathbf{R}) &= N_{NL} R^L e^{-(R/R_N)^2} Y_{LM}(\hat{\mathbf{R}}).\end{aligned} \tag{2.4}$$

The Gaussian ranges are postulated to lie in geometric progression,

$$\begin{aligned}r_n &= r_1 a^{n-1}\ (n = 1 - n_{\max}), \\ \rho_\nu &= \rho_1 \alpha^{\nu-1}\ (\nu = 1 - \nu_{\max}), \\ R_N &= R_1 A^{N-1}\ (N = 1 - N_{\max}).\end{aligned} \tag{2.5}$$

The number and ratio of range parameters for the Gaussians depends upon the spins and isospins $(l,\lambda,\Lambda,L,I,s,s',S,t)$; the explicit dependence is suppressed for simplicity of notation. Eigenenergies and wave-function coefficients C_α of the ground and excited 0^+ states are determined simultaneously by using the Rayleigh-Ritz variational

principle, namely by diagonalizing the Hamiltonian using the basis functions $\Phi_\alpha^{(\mathrm{K})}$ and $\Phi_\alpha^{(\mathrm{H})}$. In the following calculations, satisfactory convergence was obtained within $l,L,\lambda \leqslant 2$ (i.e., approximately 100 four-body angular momentum channels). However, in our variational method, the *NN* interaction is not truncated in angular momentum. Basis functions so chosen can describe accurately both short range correlations and long range asymptotic behavior simultaneously [13–15].

Diagonalization of the Hamiltonian gives rise to many discrete eigenstates other than the 0_1^+ and 0_2^+ states, so-called pseudocontinuum states, each corresponding to a superposition of continuum states in a narrow energy range around a particular eigenenergy. In Sec. IV, the $E0$ transition strengths to all 0^+ pseudocontinuum states are calculated in connection with the EW $E0$ sum rule.

III. INTERACTIONS

For the *NN* interaction we employ the AV8′ force [7], which is the same as that used in the benchmark test calculation of the ground state [6]. In this case, without including the Coulomb force, the calculated energies of the ground and the second 0^+ states are −25.90 and −7.86 MeV, respectively. The latter state is very weakly bound with respect to the calculated $3N+N$ threshold at −7.76 MeV, in agreement with Ref. [12].

In order to investigate the (e,e') form factor and the spatial structure difference between the 0_1^+ and 0_2^+ states, it is necessary to reproduce with sufficient accuracy their energies (−28.30 and −8.09 MeV) as well as the energies of ^{3}H and ^{3}He. Because the use of two-body forces alone (the AV8′ potential plus Coulomb force) does not reproduce the binding energies of the ^{3}H, ^{3}He, and ^{4}He(0_1^+), we introduce a phenomenological *NNN* force with a two-range Gaussian form,

$$\sum_{n=1}^{2} V_n^{(3)} \sum_{(ijk)} e^{-\mu_n (r_{ij}^2 + r_{jk}^2 + r_{ki}^2)}, \tag{3.1}$$

where (ijk) run over the particle numbers (1,2,3,4) cyclically in a total of four terms, r_{ij} being the distance between particles i and j. A sophisticated, spin-dependent *NNN* force is not necessary for the present purpose (to discuss the spatial structure of the 0_1^+ and 0_2^+ states); to reproduce the binding energy is essential, so that the wave functions have the correct asymptotic behavior. It is possible to adjust the *NNN* force parameters so as to reproduce simultaneously the binding energies of ^{3}H, ^{3}He, and ^{4}He(0_1^+) within the desired accuracy: a set of the parameters $\{V_1^{(3)}=-2.04$ MeV, $\mu_1 = (4.0\ \mathrm{fm})^{-2}$, $V_2^{(3)}=35.0$ MeV, $\mu_2=(0.75\ \mathrm{fm})^{-2}\}$ yield the binding energies 8.41(8.48) MeV, 7.74(7.72) MeV, and 28.44(28.30) MeV for ^{3}H, ^{3}He, and ^{4}He(0_1^+), respectively, where the observed values are shown in parentheses.

There are no additional adjustable parameters in the calculation. The issues we address are then: (i) Is the energy of the second 0^+ state reproduced?, (ii) Is the (e,e') form factor reproduced?, and (iii) Where is the major contribution to the EW $E0$ sum rule?

TABLE I. Calculated energies and specified wave-function properties of the 0_1^+ and 0_2^+ states of ^{4}He. The interactions employed are AV8′ *NN* force, the Coulomb force, and a phenomenological three-body force given by (3.1). The numbers in parentheses are experimental values. In the isospin formalism, $E(3N)$ is the average energy of ^{3}H and ^{3}He, −8.08 (−8.10) MeV.

^{4}He	0_1^+	0_2^+
E (MeV)	−28.44 (−28.30)	−8.19 (−8.09)
E-$E(3N)$ (MeV)	−20.36 (−20.20)	−0.11 (+0.01)
E_x (MeV)	0.0 (0.0)	20.25 (20.21)
P_S (%)	85.54	91.18
P_P (%)	0.38	0.08
P_D (%)	14.08	8.74
$\langle r_p^2\rangle^{1/2}$ (fm)	1.660 (1.671±0.014)	5.3
$\langle 0_2^+\lvert\Sigma_p r_p^2\rvert 0_1^+\rangle$ (fm^2)		1.38 (1.10±0.16[3])

IV. RESULTS

The calculated energies and certain wave-function properties of the ground and the second 0^+ states are summarized in Table I. For the ground state, the calculated rms charge radius, $\langle r_p^2\rangle^{1/2}$, reproduces the experimental value. The calculated energy of the second 0^+ state agrees well with the observed value. The 0_2^+ state is very weakly bound with respect to the theoretical $3N+N$ threshold, $E(3N)=-8.08$ MeV. Interestingly, the percentage probabilities of the S, P, and D components in the 0_2^+ state are almost the same as those in ^{3}H, which are $P_S=91.24\%$, $P_P=0.07\%$, and $P_D=8.70\%$ (similarly for ^{3}He). This implies that the loosely coupled $3N+N$ configuration is dominant in the second 0^+ state.

We introduce one-nucleon diagonal (transition) *mass* densities $\rho_{0_\mathrm{f}^+ 0_\mathrm{i}^+}(r)$ with $\mathrm{i,f}=1,2$,

$$\rho_{0_\mathrm{f}^+ 0_\mathrm{i}^+}(r) Y_{00}(\hat{\mathbf{r}}) = \langle 0_\mathrm{f}^+ | \frac{1}{4} \sum_{j=1}^{4} \delta(\mathbf{r}-\mathbf{r}_j) | 0_\mathrm{i}^+ \rangle, \tag{4.1}$$

where $\mathbf{r}_j$ is the position vector of jth nucleon with respect to the center-of-mass of the four nucleons. Figure 2 illustrates the mass densities of the ground and the second 0^+ states. The size of the excited state is significantly larger than that of the compact ground state. The lower panel of Fig. 2 shows the transition density between the two 0^+ states, which is explored by the (e,e') experiment.

The inelastic charge form factor, $|F_{\mathrm{inel}}(q^2)|^2$, corresponding to the transition to the 0_2^+ state, is given in the impulse approximation as

$$|F_{\mathrm{inel}}(q^2)|^2 = \frac{1}{4\pi} \left| \int e^{i\mathbf{q}\cdot\mathbf{r}} \rho_{0_1^+ 0_2^+}(r) Y_{00}(\hat{\mathbf{r}}) d\mathbf{r} \right|^2 f_\mathrm{p}(q^2), \tag{4.2}$$

where $f_\mathrm{p}(q^2)=[1/(1+0.0548q^2)]^4$ is the proton finite-size factor (q in fm^{-1}). In the range $0<q^2<2.5$ fm^{-2}, where the (e,e') data have been reported, the effect of meson exchange

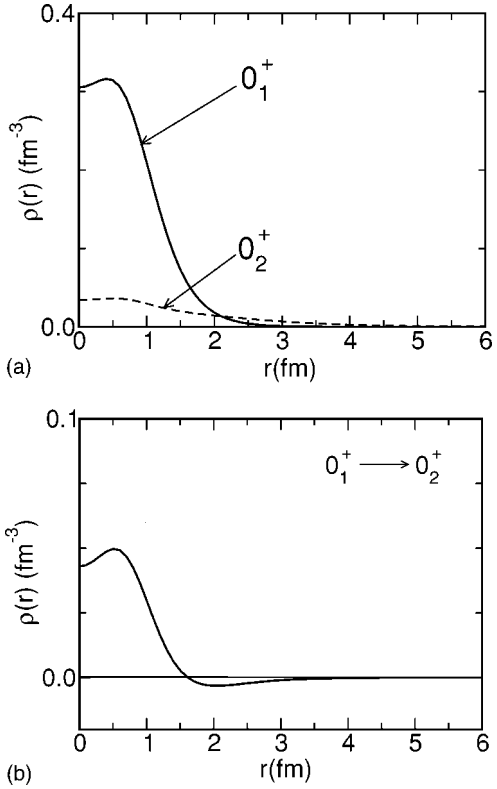

FIG. 2. Mass densities of the 0_1^+ and 0_2^+ states of ^{4}He (upper) and the transition density between them (lower).

currents is negligible [16], and our calculated elastic form factor reproduces satisfactorily that observed in Refs. [2,17,18]; e.g., $\sqrt{4\pi}|F_{\rm el}(q^2)|=0.797(0.796\pm0.025)$ at $q^2=0.5$ fm^{-2} and $0.414(0.391\pm0.012)$ at $q^2=2.0$ fm^{-2} in the calculation (observation [17]).

The observed inelastic form factor [2–4] and our calculation are shown in Fig. 3. In analogy with elastic scattering we have plotted the data of Refs. [1,4] as

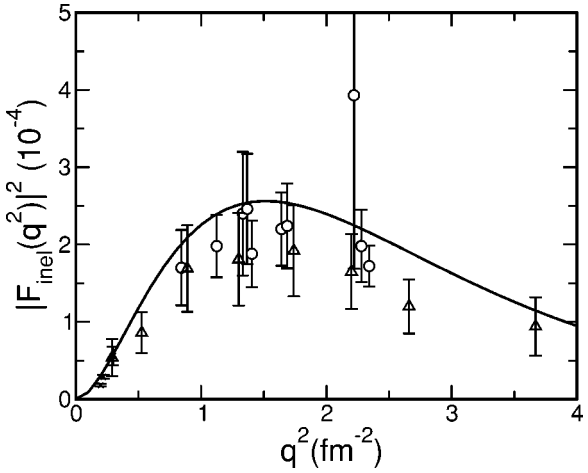

FIG. 3. Inelastic form factor for ^{4}He$(e,e')^4$He(0_2^+) from the reported four-body calculation (solid line) is compared with the available data [2–4], △, ×, and ○, respectively.

$$|F_{\rm inel}(q^2)|^2=\frac{d\sigma}{d\Omega}\Big/4\pi Z^2\frac{d\sigma}{d\Omega_{\rm Mott}}, \tag{4.3}$$

where

$$\frac{d\sigma}{d\Omega_{\rm Mott}}=\left(\frac{e^2}{2E_0}\right)\frac{\cos^2\left(\frac{1}{2}\theta\right)}{\sin^4\left(\frac{1}{2}\theta\right)\left[1+\frac{2E_0}{Mc^2}\sin^2\left(\frac{1}{2}\theta\right)\right]}, \tag{4.4}$$

with M and Z being the target mass and charge, respectively, and E_0 the incident energy. The data of Ref. [1] are included in the data reported in Ref. [2], and the cross-section data from Ref. [2] were divided by 3.2, as suggested by the reported analysis; see also Ref. [3]. The square of the form factor was obtained from Ref. [3] by multiplying $B(C0,q)$ by a factor of 4. Our values for the data appear to be similar to those reported in Ref. [5], where $|F_{\rm inel}(q^2)|^2$ in Eq. (4.3) corresponds to $|F(q^2)|$ in [4,5]. Agreement between the data and our calculation appears to be quite good. Therefore, it can be said that the drastic change in the spatial structure between the 0_1^+ to 0_2^+ states is well understood in terms of the reported four-body calculation. For a more extensive study, however, a new (e,e') measurement with smaller errors would be required. Such data would contribute significantly to few-body investigations of nuclear spatial excitations.

An effective way to investigate the spatial structure of the 0_1^+ and 0_2^+ states is to calculate the overlap amplitude between the 0^+ wave function and the ^{3}H wave function,

$$\mathcal{Y}_{0_n^+}(R_{\rm K})=\langle[\Phi_{1/2}^{(^3{\rm H})}(123)Y_0(\hat{\mathbf{R}}_{\rm K})\chi_{1/2}(4)]_{0^+}\eta_{1/2,-1/2}(4)| \times|\Psi_{0_n^+}(1234)\rangle, \tag{4.5}$$

where $\Phi_{1/2}^{(^3{\rm H})}(123)$ is the ^{3}H wave function composed of particles 1–3 and $\chi_{1/2}(4)$ and $\eta_{1/2}(4)$ are the spin and isospin wave functions of particle 4, respectively. Here $\mathbf{R}_{\rm K}$ is the position vector of particle 4 with respect to the center-of-mass of particles 1–3 (cf. *K* type of Fig. 1). The overlap amplitudes $\mathcal{Y}_{0_n^+}(R_{\rm K})$ for the 0_1^+ and 0_2^+ states are illustrated in Fig. 4. In the ground state, the fourth nucleon is located close to the other three nucleons, but it is far away from them in the second 0^+ state. (A similar result, but with a larger inner oscillation, for the 0_2^+ state was obtained by Furutani *et al.* [19] in a $3N+N$ two-cluster RGM with an effective *NN* force.) This loosely coupled $3N+N$ clustering property of the 0_2^+ state is consistent with the fact that, as mentioned above, the probability percentages of the 0_2^+ *S*, *P*, and *D* components are almost the same as those of ^{3}H (^{3}He).

Finally, we discuss the *E*0 transition and the EW *E*0 sum rule for the four-nucleon system. Let $\Sigma_p r_p^2$ denote the *E*0 operator, with r_p being the distance between a proton and the c.m. of ^{4}He with the sum running over protons. In the case where the interactions commute with the *E*0 operator, the sum rule can be written as [20]

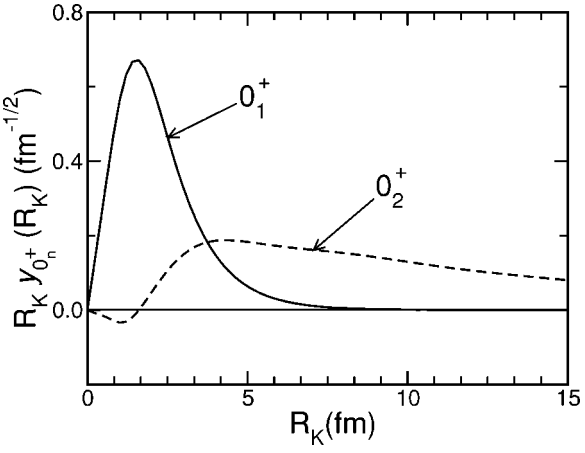

FIG. 4. The overlap amplitude between the $^4\mathrm{He}(0_n^+)$ wave function and the $^3\mathrm{H}$ wave function as defined by Eq. (4.5).

$$\sum_{n\geqslant 2}^{\infty}(E_n-E_1)\left|\langle 0_n^+|\sum_p r_p^2|0_1^+\rangle\right|^2=\frac{\hbar^2 Z}{m_N}\langle r_p^2\rangle_{0_1^+}, \qquad (4.6)$$

where E_n and $|0_n^+\rangle$ are the energy and wave function of the nth state of the four-nucleon system, respectively, m_N is the nucleon mass, and $Z=2$. Completeness is assumed for the set of states $\{|0_n^+\rangle; n=1-\infty\}$ which are normalized in a sufficiently large volume.

Calculated and observed $E0$ matrix elements are listed in the last row of Table I. The contribution from the second 0^+ state to the left-hand side (LHS) value of Eq. (4.6), the sum-rule limit, is only 11% experimentally [3] and 17% theoretically. The second 0^+ state is not a collective mode. The contribution of some 200 pseudocontinuum states above the 0_2^+ state but below $E_x=60$ MeV amounts to 70% of the LHS value. Thus, we understand that a major part of the EW $E0$ sum rule is exhausted by nonresonant, low-energy continuum states.

The reader will note that the AV8′ potential does not strictly commute with the $E0$ operator. Therefore, Eq. (4.6) does not hold; in our model space, summation in LHS saturates at $E_x\sim 300$ MeV with some 3000 pseudocontinuum states and exceeds the right-hand side (RHS) value by 4%. However, we verified that for the Minnesota *NN* force [21], which does commute with the $E0$ operator, the LHS value of Eq. (4.6) exhausts 99.9% of the RHS value with $\langle r_p^2\rangle_{0_1^+}$ calculated using the force. This means that our four-body 0^+ basis functions form an approximately complete set in our finite space and, therefore, are reliable in the investigation of the 0^+ states and the (e,e') form factor.

In conclusion, we have found that the present four-body calculation using realistic *NN* forces plus a phenomenological *NNN* force can explain the dramatic change of the spatial structure in going from the ground state to the second 0^+ state in ^{4}He. Moreover, the structure of the 0_2^+ state is primarily $3N+N$ in nature, which explains why only some 11% of the EW $E0$ sum rule is exhausted by the 0_2^+ state; the 0_2^+ state is not a monopole breathing mode.

ACKNOWLEDGMENTS

This work was supported by a Grant-in-Aid for Scientific Reseach from Monbukagakushou of Japan. E.H. acknowledges support from the Yamada Science Foundation. The research of B.F.G. is supported by the U.S. Department of Energy (Contract No. W-7405-ENG-36).

[1] R. F. Frosch, R. E. Rand, M. R. Yearian, H. Crannell, and L. R. Suelzle, Phys. Lett. **19**, 155 (1965).
[2] R. F. Frosch, R. E. Rand, H. Crannell, J. S. McCarthy, L. R. Suelzle, and M. R. Yearian, Nucl. Phys. **A110**, 657 (1968).
[3] Th. Walcher, Phys. Lett. **31B**, 442 (1970); Z. Phys. Chem. (Leipzig) **237**, 368 (1970).
[4] G. Koebschall, C. Ottermann, K. Maurer, K. Roehrich, Ch. Schmitt, and V. H. Walther, Nucl. Phys. **A405**, 648 (1983).
[5] D. Halderson, M. Yu, and J. Yu, Phys. Rev. C **39**, 336 (1989).
[6] H. Kamada, A. Nogga, W. Glöckle, E. Hiyama, M. Kamimura, K. Varga, Y. Suzuki, M. Viviani, A. Kievsky, S. Rosati, J. Carlson, S. C. Pieper, R. B. Wiringa, P. Navratil, B. R. Barrett, N. Barnea, W. Leidemann, and G. Orlandini, Phys. Rev. C **64**, 044001 (2001).
[7] B. S. Pudliner, V. R. Pandharipande, J. Carlson, S. C. Pieper, and R. B. Wiringa, Phys. Rev. C **56**, 1720 (1997).
[8] D. R. Tilly, H. R. Weller, and G. M. Hale, Nucl. Phys. **A541**, 1 (1992).
[9] H. M. Hofmann and G. M. Hale, Nucl. Phys. **A613**, 69 (1997).
[10] A. Csótó and G. M. Hale, Phys. Rev. C **55**, 2366 (1997).
[11] P. Navratil and B. R. Barrett, Phys. Rev. C **59**, 1906 (1999).
[12] A. C. Fonseca, G. Hale, and J. Haidenbauer, Few-Body Syst. **31**, 139 (2002).
[13] M. Kamimura, Phys. Rev. A **38**, 621 (1988).
[14] H. Kameyama, M. Kamimura, and Y. Fukushima, Phys. Rev. C **40**, 974 (1989).
[15] E. Hiyama, Y. Kino, and M. Kamimura, Prog. Part. Nucl. Phys. **51**, 223 (2003).
[16] M. J. Musolf, R. Schiavilla, and T. W. Donnelly, Phys. Rev. C **50**, 2173 (1994).
[17] R. F. Frosch, J. S. McCarthy, R. E. Rand, H. Crannell, and M. R. Yearian, Phys. Rev. **160**, 874 (1967).
[18] R. G. Arnold *et al.*, Phys. Rev. Lett. **40**, 1429 (1978).
[19] H. Furutani, H. Horiuchi, and R. Tamagaki, Prog. Theor. Phys. **60**, 307 (1978).
[20] R. Farrell, Phys. Rev. **107**, 1631 (1957).
[21] D. R. Thompson, M. LeMere, and Y. C. Tang, Nucl. Phys. **A268**, 53 (1977).